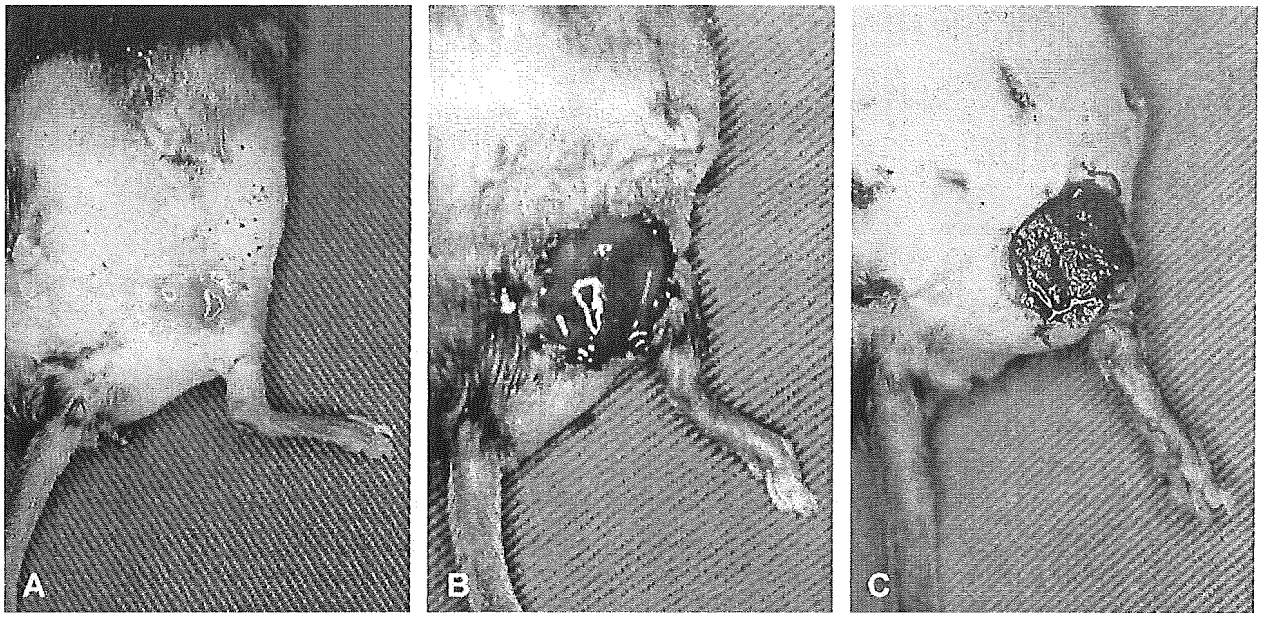

Figure 6 Tissue appearance of the wound surface, 7 days after implantation of the artificial dermis. (A) Control group, (B) single application group and (C) sustained release group.

inflammatory cells was remarkably observed in all groups because of infection. In the control group, the structure of the collagen sponge collapsed. In the sustained release group and the single application group (bFGF application groups), many new capillary formations were observed.

On day 7, all the collagen sponge were completely degraded and infiltration of the inflammatory cells was extended in the control group. Irrespective of bFGF impregnation into the microspheres, fibroblasts had infiltrated into the middle layer of the collagen sponge, and marked formation of new capillaries was observed. However, infection was observed in the single application group (Fig. 7).

Ten days after implantation, infection still remained, and numerous inflammatory cells were observed in the control group. On the other hand,

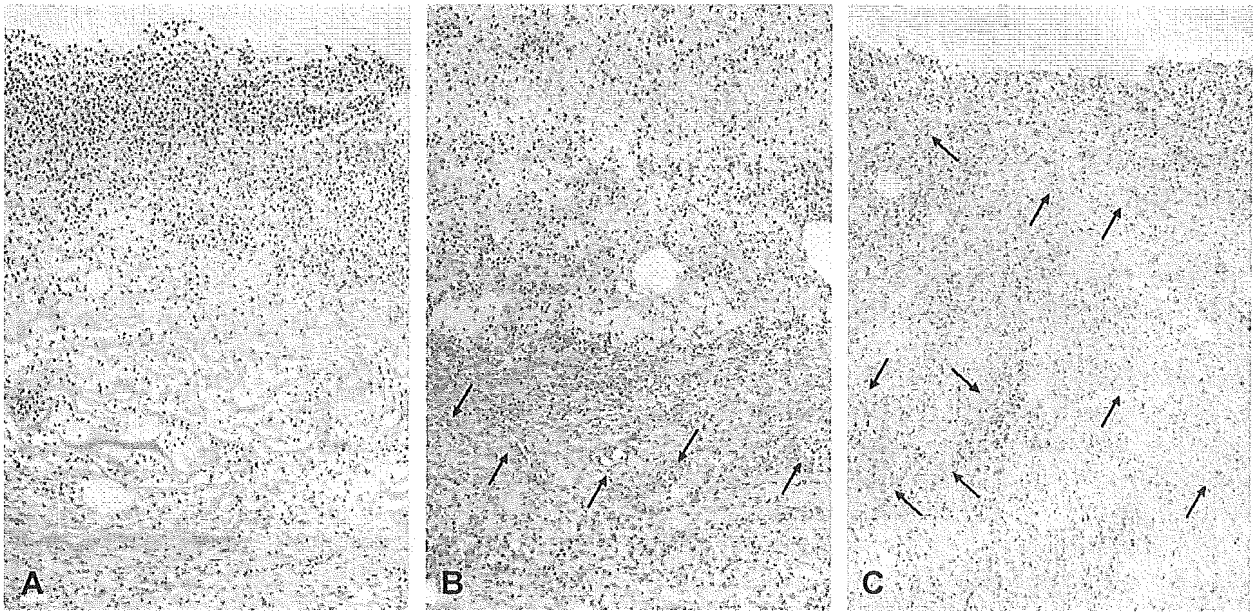

Figure 7 Histological sections of artificial dermis 7 days after implantation. (A) Control group, (B) single application group and (C) sustained release group. Haematoxylin and eosin, original magnification ×100. The arrow heads indicate new capillaries in artificial dermis.

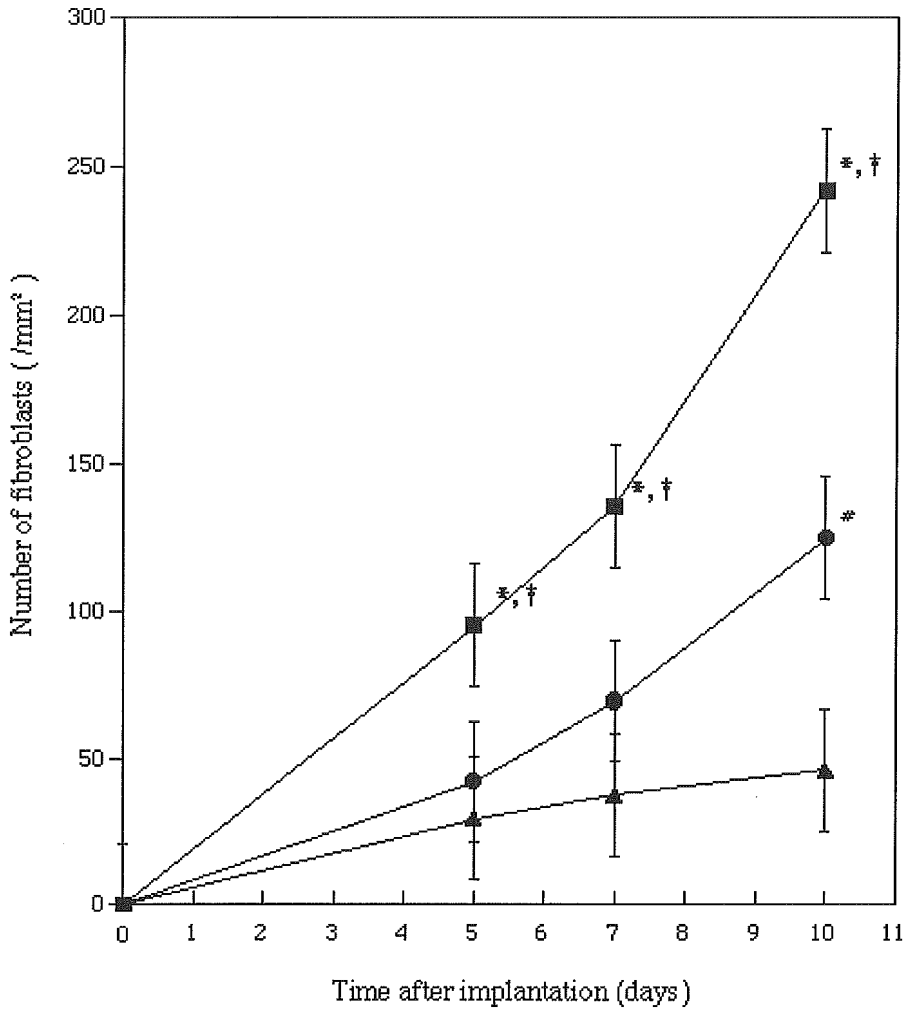

Figure 8 Time course of fibroblast proliferation. Number of fibroblasts in the sustained release group (■), the single application group (●), and the control group (▲). Each point shows the mean ± SE ($n=10$). Student's t-test was used for all statistical analyses. *$P<0.01$, compared with the control group. †$P<0.01$, compared with the single application group. #$P<0.01$, compared with the control group.

the infiltration of fibroblasts and angiogenesis were promoted in the bFGF application groups. In particular, in the sustained release group, tissue regeneration was markedly accelerated.

Proliferation of fibroblasts in the artificial dermis

Fig. 8 shows the number of fibroblasts infiltrating the artificial dermis implanted in the wound. The fibroblast number increased in a time-dependent manner in both the sustained release and single application groups. At all the times studied, the infiltration was significant in the sustained release group compared with both the single application group and the control group. No significant difference was found between the single application group and the control group after 5 or 7 days.

New capillary formation in the artificial dermis

Fig. 9 shows the number of newly formed capillaries in the artificial dermis implanted in the wound. The number of capillaries formed increased in a time-dependent manner for both the sustained release and single application groups, similarly to fibroblast proliferation. The new capillary formation was significant in both the sustained release group and single application group compared with the control group, throughout the time period studied. Five days after implantation, no significant difference

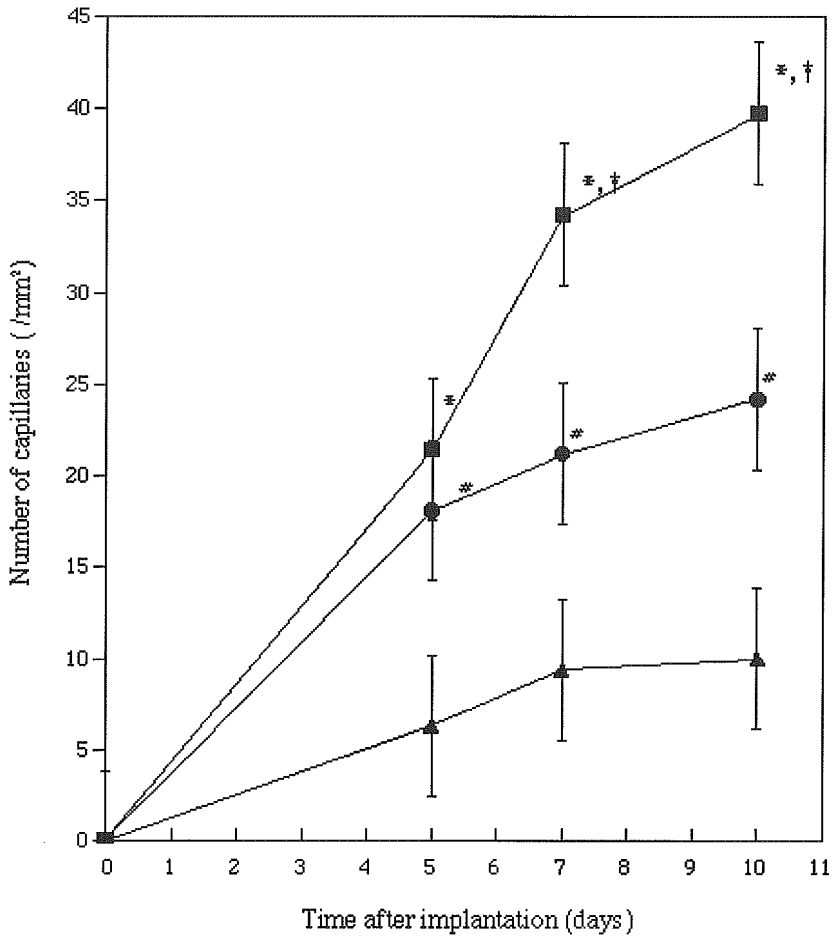

Figure 9 Time course of capillary proliferation. Number of capillaries in the sustained release group (■), the single application group (●), and the control group (▲). Each point shows the mean ± SE ($n=10$). Student's t-test was used for all statistical analyses. *$P<0.01$, compared with the control group. †$P<0.01$, compared with the single application group. #$P<0.01$, compared with the control group.

was detected between the sustained release group and the single application group. However, there was significantly new capillary formation in the sustained release group after 7 and 10 days.

Discussion

In order to accelerate wound healing, various growth factors have been studied.[1-4] Basic FGF is characterised as a growth factor for fibroblasts and capillary endothelial cells and as a potent mitogen for mesenchymal cells. Therefore, bFGF seems to be a key factor applicable to accelerate wound healing, promoting fibroblasts and inducing neovascularisation. We have also reported the effects of bFGF, and bFGF is one of the most potent angiogenic factors.[10,13] However, when bFGF is applied in solution form, it is eliminated from the applied site by simple diffusion. A radioisotope study revealed that a sustained release system is desirable to prolong the in vivo retention of bioactive bFGF.[12] A previous study demonstrated that bFGF molecules ionically complexed with the acidic gelatin were released from the microspheres as a result of gelatin biodegradation.[11]

Since its development by Yannas and colleagues[18] in 1980, artificial dermis has been used for the treatment of full-thickness skin defects resulting from burns and injuries.[19,20] We have shown that bFGF-impregnated gelatin microspheres in artificial dermis, implanted into full-thickness skin defects on the back of guinea pigs, more markedly promoted fibroblast proliferation and new capillary formation in the artificial dermis than free bFGF. In particular, the incorporation of gelatin microspheres impregnated with 50 μg of bFGF demonstrated clear efficacy.[13]

However, impaired wound healing can result clinically from problems such as diabetes, diminished circulation, and malnutrition, or from various pharmacologic agents including steroids and

immuno-suppressants. Genetically diabetic mice were chosen because they exhibit a series of characteristics similar to those of human adult onset diabetes. Wounds in these mice exhibit a marked delay in cellular infiltration, granulation tissue formation, and time required for wound closure.[16,17]

In this study, to evaluate the effect of incorporating bFGF-impregnated gelatin microspheres into an artificial dermis on impaired wound healing models, a pressure-induced decubitus ulcer was produced in these mice. The method of producing the decubitus ulcer was based on the methods described in a paper by Okumura and colleagues.[15]

After implantating the artificial dermis into the decubitus ulcer, infection was observed in all groups because diabetic mice have weak resistance to infection. Moreover, because there is no resistance in the artificial dermis,[21] when bacterial contamination occurs, the collagen sponge is not only degraded by the collagenase produced by bacteria, but also bacterial growth is promoted in the degraded collagen sponge. However, infection was gradually suppressed in the sustained group and the single application group (bFGF application groups) (Fig. 6). It was thought that the application of bFGF induced neovascularisation, and increased the resistance to infection. Kalicke et al.[22] reported that the local application of bFGF revealed the resistance to local infection. On histological examination, new capillary formation was markedly found in the bFGF application groups. In particular, it seemed that promoting neovascularisation soon after implantation was significantly effective for suppressing infection. It seemed that the sustained release of bFGF produced a better effect on the suppression of infection than a single application (Fig. 6). Therefore, in the sustained release of bFGF, the degradation of the collagen sponge was controlled and tissue regeneration in the remained matrix was also promoted. Indeed, histological examination revealed that, in the sustained release group, the proliferation of fibroblasts was significantly promoted. Degradation suppression of the collagen sponge seems advantageous from the viewpoint of tissue regeneration, because the collagen sponge functions as a good matrix for cell infiltration and proliferation. It is, therefore, appropriate that the infiltration of fibroblasts and new capillary formation were significant in the sustained release group compared with the single application group or the control group (Figs. 8 and 9). It was confirmed that bFGF-impregnated gelatin microspheres in an artificial dermis not only accelerated tissue regeneration but also increased resistance to infection.

In conclusion, bFGF accelerated dermal repair and angiogenesis in the wounds of healing-impaired diabetic mice. Accelerated tissue regeneration was achieved by greater incorporation of bFGF-impregnated gelatin microspheres than free bFGF. The effectiveness of bFGF-impregnated gelatin microspheres in an artificial dermis may be clinically useful in the treatment of patients with deficient wound repair, such as a decubitus ulcer.

References

1. Flamme I, Breier G, Risau W. Vascular endothelial growth factor (VEGF) and VEGF receptor 2 (flk-1) are expressed during vasculogenesis and vascular differentiation in the quail embryo. *Dev Biol* 1995;**169**:699-712.
2. Carter K. Growth factors: the wound healing therapy of the future? *J Community Nurs* 2003;**8**:15-23.
3. Cross KJ, Mustoe TA. Growth factors in wound healing. *Surg Clin N Am* 2003;**83**:531-45.
4. Werner S, Grose R. Regulation of wound healing by growth factors and cytokines. *Physiol Rev* 2003;**83**:835-70.
5. Asahara T, Kawamoto A. Endothelial progenitor cells for postnatal vasculogenesis. *Am J Physiol Cell Physiol* 2004; **287**:572-9.
6. Gospodarowicz D, Ferrara N, Schweigerer L. Molecular and biological characterization of fibroblast growth factor, an angiogenic factor which also controls the proliferation and differentiation of mesoderm and neuroectoderm derived cells. *Cell Differ* 1986;**19**:1-17.
7. Bikfalvi A, Savona C, Perollet C, Javerzat S. New insights in the biology of fibroblast growth factor-2. *Angiogenesis* 1998; **1**:155-73.
8. Richard J, Richard C, Daures J, Clouet S, Vannereau D, Bringer J, et al. Effect of topical basic fibroblast growth factor on the healing of chronic diabetic neuropathic ulcer of the foot. *Diabetes Care* 1995;**18**:64-9.
9. Robson MC, Hill DP, Smith PD, Wang X, Meyer-Siegler K, Ko F, et al. Sequential cytokine therapy for pressure ulcers: clinical and mechanistic response. *Ann Surg* 2000;**231**: 600-11.
10. Tabata Y, Hijikata S, Ikada Y. Enhanced vascularization and tissue granulation by basic fibroblast growth factor impregnated in gelatin hydrogels. *J Control Release* 1994;**31**: 189-99.
11. Munuruzzaman M, Tabata Y, Ikada Y. Complexation of basic fibroblast growth factor with gelatin. *J Biomater Sci Polym Ed* 1998;**9**:459-73.
12. Ymamoto M, Tabata Y, Hong L, Miyamot S, Hashimoto N, Ikada Y. Bone regeneration by transforming growth factor b1 released from a biodegradable hydrogel. *J Control Release* 2000;**64**:133-42.
13. Kawai K, Suzuki S, Tabata Y, Ikada Y, Nishimura Y. Accelerated tissue regeneration through incorporation of basic fibroblast growth factor-impregnated gelatin microspheres into artificial dermis. *Biomaterials* 2000;**21**:489-99.
14. Matuszewska B, Keogan M, Fisher DM, Soper KA, Hoe CM, Huber C, et al. Acidic fibroblast growth factor: evaluation of topical formulations in a diabetic mouse wound healing model. *Pharm Res* 1994;**11**:65-71.
15. Okumura M, Okuda T, Nakamura T, Yajima M. Effect of basic

fibroblast growth factor on wound healing in healing-impaired animal models. *Arzneim Forsch Drug Res* 1996; **46**:547-51.
16. Mizuno K, Yamamura K, Yano K, Osada T, Saeki S, Takimoto N, et al. Effect of chitosan film containing basic fibroblast growth factor on wound healing in genetically diabetic mice. *J Biomed Mater Res* 2003;**64A**:177-81.
17. Yoshida S, Matsumoto K, Tomioka D, Bessho K, Itami S, Yoshikawa K, et al. Recombinant hepatocyte growth factor accelerates cutaneous wound healing in a diabetic mouse model. *Growth Factors* 2004;**22**:111-9.
18. Yannas IV, Burke JF. Design of an artificial skin. 1. Basic design principles. *Biomed Mater Res* 1980;**14**:65-81.
19. Suzuki S, Matsuda K, Maruguchi T, Nishimura Y, Ikada Y. Further application of 'bilayer artificial skin'. *Br J Plast Surg* 1995;**48**:222-9.
20. Suzuki S, Kawai K, Ashoori F, Morimoto N, Nishimura Y, Ikada Y. Long-term follow-up study of artificial dermis composed of outer silicone layer and inner collagen sponge. *Br J Plast Surg* 2000;**53**:659-66.
21. Kawai K, Suzuki S, Tabata Y, Taira T, Ikada Y, Nishimura Y. Development of an artificial dermis preparation capable of silver sulfadiazine release. *J Biomed Mater Res* 2001;**57**: 346-56.
22. Kalicke T, Sprutacz O, Schlegel U, Kutscha-Lissberg F, Koller M, Printzen G, et al. Influence of local application of basic fibroblast growth factor on resistance to local infection after standardized closed soft tissue trauma. An experimental study in rats. *Unfallchirurg* 2004;**107**:211-8.

Graefe's Arch Clin Exp Ophthalmol
DOI 10.1007/s00417-005-0168-3

CLINICAL INVESTIGATION

Nobuyoshi Kitaichi
Tadamichi Shimizu
Ayumi Honda
Riichiro Abe
Kazuhiro Ohgami
Kenji Shiratori
Hiroshi Shimizu
Shigeaki Ohno

Increase in macrophage migration inhibitory factor levels in lacrimal fluid of patients with severe atopic dermatitis

Received: 28 April 2005
Revised: 17 September 2005
Accepted: 18 September 2005

N. Kitaichi (✉) · K. Ohgami · K. Shiratori · S. Ohno
Department of Ophthalmology and Visual Sciences,
Hokkaido University Graduate School of Medicine,
060-8638, Sapporo, Japan
e-mail: nobukita@med.hokudai.ac.jp

T. Shimizu · A. Honda · R. Abe · H. Shimizu
Department of Dermatology,
Hokkaido University Graduate School of Medicine,
060-8638, Sapporo, Japan

Abstract *Background and aims of the study:* Atopic dermatitis is a chronic inflammatory skin disorder that often involves some ophthalmic features. Macrophage migration inhibitory factor (MIF) is a proinflammatory cytokine that is associated with the generation of cell-mediated immune responses. Although serum MIF levels may be elevated in severe atopic dermatitis, the quantity of MIF in regional ocular fluid remains unknown. We measured MIF levels in tears (lacrimal fluid) of patients with atopic dermatitis. *Patients and methods:* Tear samples were collected from 16 patients with atopic dermatitis, 10 patients with allergic conjunctivitis, and 15 healthy control subjects. The clinical severity of atopic dermatitis was evaluated according to the Scoring Atopic Dermatitis (SCORAD) index. The index was calculated by summing the following scores: extent criteria, intensity criteria, and subjective symptoms. Macrophage migration inhibitory factor levels were determined by a human MIF enzyme-linked immunosorbent assay. All comparisons were two-tailed, and P values <0.01 were considered as statistically significant. *Results:* The mean MIF concentration in lacrimal fluid collected from healthy control subjects was 0.69± 0.2 ng/ml. The mean tear MIF levels were 17.87± 6.3 ng/ml in moderate-to-severe atopic dermatitis (SCORAD≥ 15, P=0.002), 0.93±0.08 ng/ml in mild atopic dermatitis (SCORAD< 15), and 2.76± 0.86 ng/ml in allergic conjunctivitis (P=0.008). *Conclusions:* A proinflammatory cytokine MIF level was elevated in tears as well as serum in cases of severe atopic dermatitis. These results suggest that MIF may play an important role in the induction or enhancement of ophthalmic features related to severe atopic dermatitis.

Keywords Allergic conjunctivitis · Atopic dermatitis · Eye · MIF · Serum · Tears

Introduction

Macrophage migration inhibitory factor (MIF) was first discovered in the late 1960s; it is therefore believed to be the first recognized lymphokine [6]. Since MIF was discovered as merely a part of the phenomenon of inhibiting migration of macrophages in the pre-molecular biology era, many scientists doubted its importance in the immune response. Investigations in the 1990s aimed at identifying novel systemic mediators that could regulate host inflammatory responses led to the identification of murine MIF as a product secreted by the anterior pituitary gland [2]. Upon stimulation, T cells release MIF, and MIF activity was first described as a product of cognate T-cell supernatants [15]. Macrophages have also been identified as an important source of MIF and are known to express MIF both constitutively and upon stimulation [15]. Macrophage migration inhibitory factor is considered to act by both paracrine and autocrine stimulatory pathways to augment the activation of these cells [15]. As reported

previously, MIF is essential for T-cell activation and possibly contributes to maintaining Th1/Th2 imbalance [1]. Increased MIF expression has been reported in lesions from many immune/inflammatory diseases, including psoriasis, glomerulonephritis, transplant rejection, neuro-Behçet's disease, asthma, adult respiratory distress syndrome, and inflammatory eye diseases [3, 4, 7, 11–13, 16, 17, 20, 22, 24].

Atopic dermatitis (AD) frequently involves some ophthalmic features: blepharitis, chronic keratoconjunctivitis, keratoconus, early-onset cataract, and rarely, retinal detachment [9]. AD is a chronic inflammatory skin disorder and many reports have documented its pathogenesis in relation to genetic and immunological abnormalities as well as environmental factors [10]. Although abnormal populations of Th1 and Th2 subsets of helper T cells (Th1/Th2 imbalance) have been identified as a cause of the pathogenesis of AD [8, 13, 25], a decrease in delayed-type hypersensitivity (DTH) is considered to involve more than Th1/Th2 imbalance in AD [5]. MIF is essential for T-cell activation and possibly contributes to maintaining Th1/Th2 imbalance as described above [1]. Also, a prominent increase in systemic MIF levels was detected in patients with severe AD, and the levels decreased when the clinical symptoms improved following treatment with corticosteroid ointment [18, 19]. We hypothesized that a high concentration of MIF could exist in the regional fluid of the eye as well as in serum in cases of severe atopic dermatitis. Because the Scoring Atopic Dermatitis (SCORAD) index, which is determined on the basis of several criteria related to lesion spread and intensity as well as on subjective signs, is commonly used to evaluate AD [21], AD patients were classified into two groups, as moderate-to-severe or mild AD, according to SCORAD index in the present study. We measured the MIF levels in tears (lacrimal fluid) of patients with AD and compared them to those of patients with allergic conjunctivitis (AC) and healthy people.

Materials and methods

Patients

We studied 16 patients with AD and 9 subjects with AC who visited the Departments of Dermatology and Ophthalmology, Hokkaido University Hospital, Sapporo, Japan. Atopic dermatitis is a common inflammatory disorder characterized by a chronic and relapsing course. In order to evaluate the severity of the disease as objectively as possible, the European Task Force on Atopic Dermatitis developed a method allowing consistent assessment by means of a severity index, called the Scoring Atopic Dermatitis (SCORAD) index [21]. The index should be calculated as a sum of the following scores: (1) extent criteria (involved surface area), (2) intensity criteria (erythema, edema/papulation, oozing/crusting, excoriation, and lichenification), and (3) subjective symptoms (pruritus and insomnia) [21]. We classified cases of AD in this study as "moderate-to-severe" (SCORAD≥15) or "mild" (SCORAD<15) according to the SCORAD index. Each patient with moderate-to-severe AD had atopic manifestations on the facial skin. Allergic conjunctivitis (AC) was diagnosed by slit lamp examination according to the guidelines of diagnosis and treatment of conjunctivitis, reported elsewhere [23]. Although we collected tear samples out of pollen season (December, January, and February), five of ten AC patients stated that they had sensitivity to grass or birch pollen. Most of the AC patients were considered to be in the chronic phase of AC, and their conjunctival signs and symptoms were mild. Tear samples were collected from 9 patients with severe AD (mean age, 26.1 years; age range, 18–37 years), 7 patients with mild AD (mean age, 29.0 years; age range, 16–44 years), 10 patients with AC (mean age, 32.6 years; age range, 22–44 years), and 15 healthy volunteers (mean age, 34.6 years; age range, 23–45 years). All subjects were Japanese, and healthy volunteers with no history of AD were recruited from our colleagues as controls. Dermatologists and ophthalmologists also verified no manifestations of AD and AC in controls when their tear/serum samples were collected. Informed consent was obtained from every patient and control subject.

Collection of tears and sera

All of the experiments in this study followed the tenets of the Declaration of Helsinki. After informed consent was obtained, tear samples were collected from all subjects. To obtain unstimulated basal lacrimal fluid, the tear samples (10 μl) were collected with microcapillary tubes for microhematocrit (75 mm length, Funakoshi, Tokyo) at the lateral canthus of patients in the supine position without any anesthesia. After obtaining informed consent, serum samples were collected from two of the severe AD patients whose tear MIF levels were quite high (>27.2 ng/ml), exceeding one standard deviation (SD) from the group's median value. Also, two subjects were chosen randomly from the patients with mild AD and healthy controls to measure their serum MIF levels.

Tear samples were centrifuged immediately at 4°C to remove cells and transferred into new tubes. Tear and serum samples were stored at −80°C until further examination.

Measurement of MIF

Macrophage migration inhibitory factor levels were determined by a human MIF enzyme-linked immunosorbent assay (ELISA) (CosmoBio, Tokyo, Japan) as described previously [18]. The kit contains all reagents necessary for performing the assay. Statistical analysis was performed using the Mann-Whitney U test.

Table 1 Values and significance of MIF levels in tears

	MIF levels (Mean MIF±SE)	*P* values vs. normal
Normal controls	0.69±0.2	-
AD: moderate to severe	17.87±6.3	0.002**
AD: mild	0.93±0.08	0.07
Allergic conjunctivitis	2.76±0.86	0.008**

AD Atopic dermatitis
**$P<0.01$ (Mann-Whitney U test, two-tailed)

Results

The mean MIF level in lacrimal fluid collected from healthy control subjects was 0.69±0.2 ng/ml. The mean tear MIF levels were 17.87±6.3 ng/ml in cases of moderate-to-severe AD (SCORAD≥15), 0.93±0.08 ng/ml in cases of mild AD (SCORAD<15), and 2.76±0.86 ng/ml in cases of allergic conjunctivitis (AC). Tear MIF levels were significantly elevated in patients with moderate-to-severe AD compared to normal controls (P=0.002, Table 1). The tear MIF levels of patients with AC were also higher than those of healthy subjects (P=0.008, Table 1). We did not, however, detect any significant difference in tear MIF levels between patients with mild AD (SCORAD<15) and healthy control subjects (P=0.07, Table 1).

We then focused on two cases of severe AD in which the tear MIF levels were higher than 27.2 ng/ml, i.e., more than one standard deviation (SD) from the group's median value. Both had the severest skin manifestations of atopic dermatitis in this study when their tears were collected. After informed consent was obtained from these patients, serum samples were drawn and the serum MIF levels were measured. As shown in Table 2, their serum MIF levels were approximately equivalent to those in the lacrimal fluid of patients with severe AD. In contrast, although the serum MIF levels in cases of mild AD were still elevated compared to those of healthy controls, their MIF concentrations in tears were no higher than those of healthy controls (Table 2).

Table 2 MIF concentrations of tears and sera

Cases	Age/sex	Tear MIF (ng/ml)	Serum MIF (ng/ml)
1. AD: severe	20/M	63.4	79.7
2. AD: severe	35/M	30.1	42.0
3. AD: mild	44/F	0.9	17.5
4. AD: mild	16/M	0.7	12.2
5. Control	45/F	0.8	4.7
6. Control	24/F	1.0	3.2

AD Atopic dermatitis

Discussion

In the present study, we detected high levels of MIF in the lacrimal fluid of patients with severe AD. We previously reported an increase in serum MIF levels in patients with AD [18]. Although AD frequently involves some ophthalmic features (blepharitis, chronic keratoconjunctivitis, keratoconus, early-onset cataract, and retinal detachment), how MIF behaves in the ocular fluid of patients with AD remained unknown. We wished to determine how tear MIF levels of patients with severe AD compared with AC and healthy subjects.

MIF is expressed and secreted in many tissues: in the brain, eye (lens, corneal epithelial cells, iris, ciliary body, and retina), ear, immune cells (thymus, spleen, lymph nodes, blood, and bone marrow, by monocytes, macrophages, T cells, B cells, dendritic cells, eosinophils, basophils, neutrophils, and mast cells), lungs, breast, endocrine systems (pituitary gland, adrenal cortex, and pacreas), liver, testis, prostate, ovaries, gastrointestinal tract, kidney, fat tissue, skin (by keratinocytes, sebaceous glands, hair follicles, endothelial cells and fibroblasts), bone, and joints [4]. This study demonstrated that tear MIF concentration is significantly higher in patients with severe AD than in controls. Patients with AC also showed significantly higher levels of MIF than healthy controls; however, there were vast differences between the averages of AD and AC groups.

Since MIF levels in tears were elevated for both diseases involving the immune system, one possible source of tear MIF is the lymphocytes in conjunctival follicles. Another possible cause of the elevation of tear MIF levels in the eyes may be the lacrimal gland, but no study has been performed to determine if the lacrimal gland expresses or secretes MIF or not. A third possible source may be peripheral blood mononuclear cells (PBMCs) [14]. As previously reported, a substantial increase in systemic MIF levels was detected in patients with severe AD, and the levels decreased when the skin symptoms improved following treatment with corticosteroid ointment [18]. Furthermore, the elevated serum MIF was due to secretion from systemic PBMC [18, 19]. We found two patients with severe AD who showed extremely high levels (in excess of 30 ng/ml) of MIF in this study. To examine how blood PBMC contributes to MIF levels in lacrimal fluid, we collected serum samples from AD patients as well as tears. Because a very high serum MIF concentration was detected in both of these patients (Table 2) and the space of the oculi is limited, some proportion of MIF in tears may be attributable to a systemic increase in MIF. The secretion of MIF from PBMCs might contribute to the elevation of tear MIF levels more than regional inflammatory cells of the eyes in patients with severe AD. Since we did not collect blood samples from AC subjects, it is still unclear how much blood PBMC contributes to tear MIF levels in cases of AC. In the present study, AC patients did not have

obvious systemic inflammation, but local. Moreover, we detected higher tear MIF levels in the AC group than in the mild AD group, suggesting that MIF may be secreted in the eye to some extent. Further studies might be required in vernal or other etiologies of conjunctivitis, as well as for treated vs. untreated AC to clarify eye-derived MIF in tears.

This is the first report that MIF concentrations in tears are elevated in cases of severe AD in humans. In conclusion, MIF in regional ocular fluid may be involved in the induction or enhancement of ophthalmic features caused by severe AD.

Acknowledgements The authors are grateful to Dr. Hiroshi Fujishima and Dr. Kazumi Fukagawa (Department of Ophthalmology, Tokyo Dental College, Ichikawa, Japan) for their technical cooperation. This study was supported by a Grant-in-Aid for Research from the Ministry of Education, Culture, Sports, Science, and Technology (MEXT) Japan, a Grant for Research on Sensory and Communicative Disorders from The Ministry of Health, Labor, and Welfare, Japan, and by Research Fellowships of Japan Society for the Promotion of Science (JSPS) for Young Scientists.

References

1. Bacher M, Metz CN, Calandra T, Mayer K, Chesney J, Lohoff M, Gemsa D, Donnelly T, Bucala R (1996) An essential regulatory role for macrophage migration inhibitory factor in T-cell activation. Proc Natl Acad Sci USA 93 (15):7849–7854
2. Bernhagen J, Calandra T, Mitchell RA, Martin SB, Tracey KJ, Voelter W, Manogue KR, Cerami A, Bucala R (1993) MIF is a pituitary-derived cytokine that potentiates lethal endotoxaemia. Nature 365 (6448):756–759
3. Brown FG, Nikolic-Paterson DJ, Chadban SJ, Dowling J, Jose M, Metz CN, Bucala R, Atkins RC (2001) Urine macrophage migration inhibitory factor concentrations as a diagnostic tool in human renal allograft rejection. Transplantation 71 (12):1777–1783
4. Calandra T, Roger T (2003) Macrophage migration inhibitory factor: a regulator of innate immunity. Nat Rev Immunol 3 (10):791–800
5. Cooper KD (1994) Atopic dermatitis: recent trends in pathogenesis and therapy. J Invest Dermatol 102 (1):128–137
6. David JR (1966) Delayed hypersensitivity in vitro: its mediation by cell-free substances formed by lymphoid cell-antigen interaction. Proc Natl Acad Sci USA 56 (1):72–77
7. Donnelly SC, Haslett C, Reid PT, Grant IS, Wallace WA, Metz CN, Bruce LJ, Bucala R (1997) Regulatory role for macrophage migration inhibitory factor in acute respiratory distress syndrome. Nat Med 3 (3):320–323
8. Holden CA (1993) Atopic dermatitis-messengers, second messengers and cytokines. Clin Exp Dermatol 18 (3):201–207
9. Kanski JJ (2003) Clinical Ophthalmology, a systematic approach, 5th edn. Buttherworth-Heinemann/ Elsevier Science, Edinburgh, UK
10. Kapp A (1995) Atopic dermatitis-the skin manifestation of atopy. Clin Exp Allergy 25 (3):210–219
11. Kitaichi N, Kotake S, Mizue Y, Matsuda H, Onoé K, Nishihira J (2000) Increase of macrophage migration inhibitory factor in sera of patients with iridocyclitis. Br J Ophthalmol 84 (12):1423–1425
12. Kitaichi N, Kotake S, Sasamoto Y, Namba K, Matsuda A, Ogasawara K, Onoé K, Matsuda H, Nishihira J (1999) Prominent increase of macrophage migration inhibitory factor in the sera of patients with uveitis. Invest Ophthalmol Vis Sci 40 (1):247–250
13. Lan HY, Yang N, Nikolic-Paterson DJ, Yu XQ, Mu W, Isbel NM, Metz CN, Bucala R, Atkins RC (2000) Expression of macrophage migration inhibitory factor in human glomerulonephritis. Kidney Int 57 (2):499–509
14. Lever R, Turbitt M, Sanderson A, MacKie R (1987) Immunophenotyping of the cutaneous infiltrate and of the mononuclear cells in the peripheral blood in patients with atopic dermatitis. J Invest Dermatol 89 (1):4–7
15. Morand EF, Bucala R, Leech M (2003) Macrophage migration inhibitory factor: an emerging therapeutic target in rheumatoid arthritis. Arthritis Rheum 48 (2):291–299
16. Niino M, Ogata A, Kikuchi S, Tashiro K, Nishihira J (2000) Macrophage migration inhibitory factor in the cerebrospinal fluid of patients with conventional and optic-spinal forms of multiple sclerosis and neuro-Behcet's disease. J Neurol Sci 179 (S 1–2):127–131
17. Rossi AG, Haslett C, Hirani N, Greening AP, Rahman I, Metz CN, Bucala R, Donnelly SC (1998) Human circulating eosinophils secrete macrophage migration inhibitory factor (MIF). Potential role in asthma. J Clin Invest 101 (12):2869–2874
18. Shimizu T, Abe R, Ohkawara A, Mizue Y, Nishihira J (1997). Macrophage migration inhibitory factor is an essential immunoregulatory cytokine in atopic dermatitis. Biochem Biophys Res Commun 240 (1):173–178
19. Shimizu T, Abe R, Ohkawara A, Nishihira J (1999) Increased production of macrophage migration inhibitory factor by PBMCs of atopic dermatitis. J Allergy Clin Immunol 104 (3 Pt 1): 659–664
20. Shimizu T, Nishihira J, Mizue Y, Nakamura H, Abe R, Watanabe H, Ohkawara A, Shimizu H (2001) High macrophage migration inhibitory factor (MIF) serum levels associated with extended psoriasis. J Invest Dermatol 116 (6):989–990
21. Stadler J (1993) Severity scoring of atopic dermatitis: the SCORAD index. Consensus report of the European Task Force on Atopic Dermatitis. Dermatology 186 (1):23–31
22. Sustiel A, Rocklin R (1989) T cell responses in allergic rhinitis, asthma and atopic dermatitis. Clin Exp Allergy 19 (1):11–18
23. Uchio E, Ono SY, Ikezawa Z, Ohno S (2000) Tear levels of interferon-gamma, interleukin (IL) -2, IL-4 and IL-5 in patients with vernal keratoconjunctivitis, atopic keratoconjunctivitis and allergic conjunctivitis. Clin Exp Allergy 30 (1):103–109
24. Yamaguchi E, Nishihira J, Shimizu T, Takahashi T, Kitashiro N, Hizawa N, Kamishima K, Kawakami Y (2000) Macrophage migration inhibitory factor (MIF) in bronchial asthma. Clin Exp Allergy 30 (9):1244–1249
25. Zachary CB, Allen MH, MacDonald DM (1985) In situ quantification of T-lymphocyte subsets and Langerhans cells in the inflammatory infiltrate of atopic eczema. Br J Dermatol 112 (2):149–156

Volume 54(1): 109–118, 2006
Journal of Histochemistry & Cytochemistry
http://www.jhc.org

ARTICLE

Colocalization of Multiple Laminin Isoforms Predominantly beneath Hemidesmosomes in the Upper Lamina Densa of the Epidermal Basement Membrane

James R. McMillan, Masashi Akiyama, Hideki Nakamura, and Hiroshi Shimizu

Creative Research Initiative Sousei (JRM) and Department of Dermatology, Graduate School of Medicine (JRM,MA,HN,HS), Hokkaido University, Sapporo, Japan

SUMMARY Multiple laminin isoforms including laminins 5 (α3 β3 γ2), 6 (α3 β1 γ1), 10 (α5 β1 γ1), and possibly laminins 7 (α3 β2 γ1) and 11 (α5 β2 γ1) are present in the epidermal basement membrane. However, only the precise epidermal ultrastructural localization of laminin 5 (α3 β3 γ2) has been elucidated. We therefore determined the precise expression and ultrastructural localization of the α5, β1, β2, and γ1 chains in the epidermis. The expression of laminin chains in skin samples was analyzed from patients with epidermolysis bullosa (EB, n=15) that harbor defects in specific hemidesmosome (HD)-associated components. The expression of the α5, β1, and γ1 chains (present in laminins 10/11) and β2 chain (laminins 7/11) was unaffected in all intact (unseparated) skin of EB patients including Herlitz junctional EB with laminin-5 defects (n=6). In the basement membrane of human epidermis, the α5, β1, β2, and γ1 chains were expressed but also localized to the dermal vessels. Immunogold electron microscopy of normal human epidermis localized the α5, β1, β2, and γ1 chains to the upper lamina densa, with between 84% and 92% of labeling restricted to beneath the HDs, similar to laminin 5 (n≥200 gold particles per sample, sample number n=4) but distinct from collagen IV labeling (with only 63% labeling beneath HDs, p<0.001). Taken together, the majority of the α5β1/β2γ1 laminin chains are located beneath HDs. This suggests that laminin-10-associated chains have specific functions or molecular interactions beneath HDs in the epidermal basement membrane.

(J Histochem Cytochem 54:109–118, 2006)

KEY WORDS
anchoring filament
epidermal basement membrane
hemidesmosome
immunoelectron microscopy
laminin 5
laminin 10

IN SKIN, laminins are present in the epidermal basement membrane, around blood vessels, nerves, and adnexal structures. It is generally thought that laminin 5 (α3 β3 γ2), possibly laminin 6 (α3 β1 γ1), and laminin 10 (α5 β1 γ1) are expressed in the human epidermal basement membrane (Aumailley and Rousselle 1999) (see Figure 1). The expression of laminins 7 (α3 β2 γ1) and 11 (α5 β2 γ1) has yet to be confirmed in the adult human epidermis (Aumailley and Rousselle 1999). Of these, laminin 5 (α3 β3 γ2) is the most well-studied epidermal isoform (Nishiyama et al. 2000; Mercurio et al. 2001; Geuijen and Sonnenberg 2002; McMillan et al. 2003b). Laminin 5 is thought to be crucial for the correct assembly and adhesion of hemidesmosomes (HDs) via the receptor, the α6β4 integrin (Niessen et al. 1994).

The distinct roles of laminin isoforms in the processes of cutaneous morphogenesis are poorly understood. Laminin 10 (α5 β1 γ1), however, has recently been implicated in several functions including hair follicle development (Li et al. 2003). In an α5 chain (laminin 10/11) knockout mouse model, the addition of exogenous laminin 10 was used to correct follicular development (Li et al. 2003). Laminin 10 is therefore implicated in hair follicle cell growth and adhesion (Gu et al. 2001; Pouliot et al. 2002; Li et al. 2003). Cell adhesion assays have demonstrated that multiple laminins (including laminins 5, 10, and 11) can act as adhesive substrates for keratinocytes and that this adhesion is mediated by the integrins α3β1 and α6β4

Correspondence to: James R. McMillan, MSc, PhD, Department of Dermatology, Hokkaido University Graduate School of Medicine, Kita-ku, Sapporo, 060-8638, Japan. E-mail: jrm57@med.hokudai.ac.jp

Received for publication March 28, 2005; accepted September 6, 2005 [DOI: 10.1369/jhc.5A6701.2005].

 0022-1554/05/$3.30

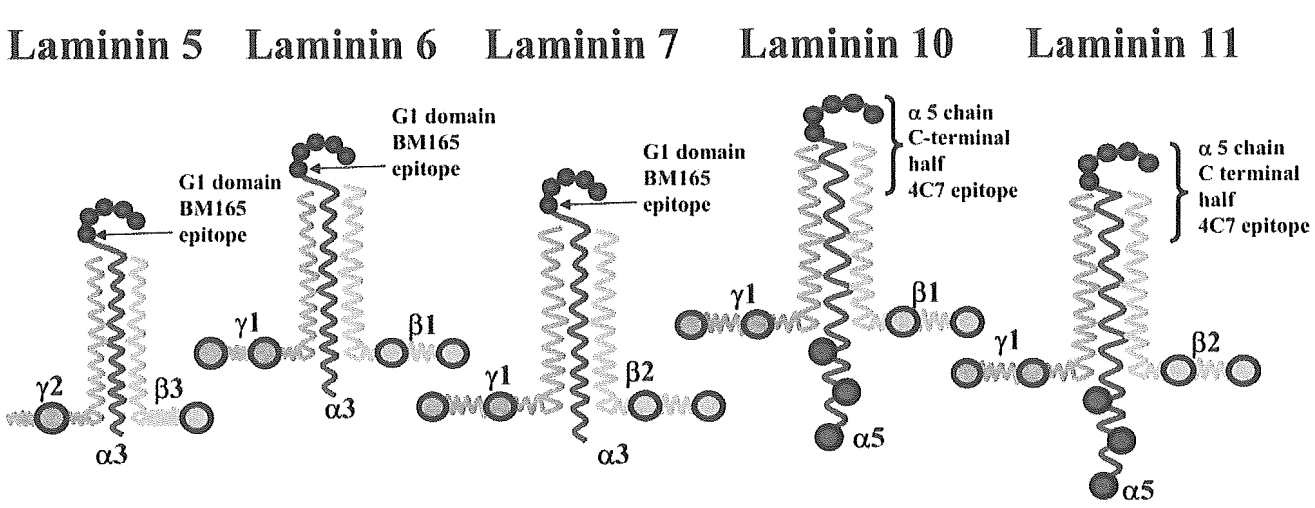

Figure 1 Schematic diagram showing the structure of laminin 5 and 10 chains and the position of two antibody binding sites in the α3 chain G1 domain (BM165) and the carboxyl terminal half of the α5 chain (4C7). This schematic diagram is not drawn to scale and does not include any α3 chain splice variants of laminin 5 (α3 β3 γ2). The antibody BM165 binds to the first globular (G1) domain of the α3 chain of laminins 5/6 (McMillan et al. 2003b), whereas the antibody 4C7 binds to the carboxyl terminal half end of the α5 chain (present in both laminins 10 and 11).

(Pouliot et al. 2002). However, in certain non-epithelial cells, the integrins α3β1, α6β1, and α6β4 and α dystroglycan are expressed and have been identified as possible laminin 10/11 receptors (Kikkawa et al. 1998, 2000; Yu and Talts 2003).

Antibodies are now available that recognize specific laminin chains and provide new tools to investigate the structure of the epidermal basement membrane. These antibodies include 4C7 (Engvall et al. 1990; Tiger et al. 1997) that recognizes a carboxyl terminal domain of the human α5 chain of laminins 10 (α5 β1 γ1, see Figure 1) and 11 (α5 β2 γ1). This antibody blocks the epitope involved in neurite cell adhesion to the laminin α5 chain (Engvall et al. 1986; Makino et al. 2002). Further laminin-specific antibodies to β and γ chains include 2E8 (recognizing the β1 chain (Engvall et al. 1986), D18 (γ1) (Sanes et al. 1990), and C4 (β2) (Hunter et al. 1989).

To better understand the position and possible functions of epidermal molecules, we examined the precise localization of the α5, β1, β2, and γ1 laminin chains and collagen IV in the interfollicular and follicular epidermal basement membrane. In addition, the expression of laminin chains was also assessed in a range of epidermolysis bullosa (EB) patients' skin harboring defects in several basement membrane components, including laminin 5. We have quantitatively analyzed and compared the localizations of laminin α5, β1, β2, and γ1 chains with that of laminin 5 (α3 β3 γ2) from our previously published data (McMillan et al. 2003b) and collagen IV. Comparison of α5, β1, β2, and γ1 chain expression with laminin 5, a well-studied HD-associated isoform, will determine a more precise localization for these laminin isoforms. Our data support the hypothesis that multiple laminin isoforms colocalize beneath HDs in normal and diseased epidermal basement membranes.

Materials and Methods

Skin Samples

Samples of adult and neonatal control skin from non-specialized sites (abdomen, arm, thigh, $n=8$; and scalp skin, $n=2$) were obtained from routine surgical procedures. Skin samples were frozen for cryostat sectioning or processed for post-embedding immunogold electron microscopy (IEM) as described below. In all cases, the biopsies were performed with the patient's or guardian's informed consent, with the relevant institutional approval for experiments handling human material, and in accordance with the Helsinki Declaration.

Skin samples from patients affected with a group of rare genodermatoses, EB, were included in this study ($n=15$, see Table 1). Details of the number of patients for each EB disease subtype, their age at biopsy, details of any identified mutations, or significant results of diagnostic antibody staining are listed, in addition to the results of their laminin antibody staining findings (see Table 1). Four Herlitz junctional (HJ) EB patients harbored laminin-5 chain mutations that were reported in the literature (Takizawa et al. 1998a–d). In one EB simplex associated with muscular dystrophy (EBS-MD) patient, genetic defects have been reported (Pulkkinen et al. 1996).

Confocal Immunofluorescence Microscopy

Indirect immunofluorescence was performed as previously described (Kennedy et al. 1985) using cryostat skin sections. Laminin chain expression was confirmed in control skin using the following antibodies: 4C7 recognizing the human α5 chain (see Figure 1) present in laminins 10 and 11 (dilution

Table 1 Comparison of laminin 5 and laminin 10 expression in patients with various forms of epidermolysis bullosa

EB disease subtype	Deficient protein	Patients' sex, age, mutation, and staining details	Laminin-5 γ3 chain GB3 expression	Laminin-10 α5 chain 4C7 expression
Control (5)	Normal	M/31 years, 33 years, 41 years, 45 years, F/15 years	+++	+++
HJEB (6)	Laminin 5	M/1 month, W610X/Q166X LAMB3	−	+/++
		F/9 months, 1997-2A>C (homozygous, LAMB3)		
		F/1 month, Q936X LAMB3		
		M/1 month, 1929delCA/W610X LAMB3		
		F/2 months, M/1 month, laminin-5 negative (GB3 moAb)		
NHJEB (2)	Laminin 5	M/12 years, M/5 years, laminin-5 reduced (GB3 moAb)	+	+++
NHJEB (2)	Collagen XVII	M/21 years, F/35 years, G252X collagen XVII negative (233, 1A8C moAb)	+++	+++
SRDEB (2)	Collagen VII	M/7 years, M/1 year, collagen VII negative (LH7:2 moAb)	+++	+++
JEB-PA/PA-EBS (1)	Integrin α6β4	F/1 month, α6β4 integrin negative (3E1,GOH3 moAb)	+++	+++
EBS-MD (2)	Plectin	M/27 years, M/9 years, plectin negative (HD1-121 moAb)	+++	+++

EB, epidermolysis bullosa; HJEB, Herlitz junction epidermolysis bullosa; NHJEB, non-Herlitz junctional epidermolysis bullosa; SRDEB, severe recessive dystrophic epidermolysis bullosa; JEB-PA, junctional epidermolysis bullosa associated with pyloric atresia; which is also known as EBS-PA, epidermolysis bullosa associated with pyloric atresia. +++, normal, bright staining pattern along dermal–epidermal junction; ++, reduced dermal–epidermal junction staining compared to controls; +, severely reduced dermal–epidermal junction staining compared to controls; −, absent dermal–epidermal junction staining compared to controls.

1:25; Chemicon International, Temecula, CA) (Engvall et al. 1990; Tiger et al. 1997). The monoclonal antibody 2E8 recognizing the β1 chain (neat) (Engvall et al. 1986), the monoclonal antibody D18 that recognizes the γ1 chain (see Figure 1) (neat) (Sanes et al. 1990), and an antibody C4 to the β2 chain (see Figure 1) (used neat) (Hunter et al. 1989) were also included. The antibodies 2E8, D18, and C4 were obtained from the Developmental Studies Hybridoma Bank, University of Iowa (Iowa City, IA). The mouse monoclonal M3F7 recognizing the helical domain of the α1 and α2 chains of collagen IV (used neat) (Foellmer et al. 1983) was also obtained from the Developmental Studies Hybridoma Bank. Laminin-5 antibodies included the mouse monoclonal BM165 directed against the laminin-5 α3 chain terminal first globular (G1) domain (see Figure 1) (diluted 1:50) (Marinkovich MP, unpublished data) (McMillan et al. 2003b); K140 directed against the laminin-5 β3 chain adjacent to domain IV; GB3 directed against the laminin-5 γ2 chain (Harlan Sera Lab; Loughborough, UK); and a rabbit polyclonal serum directed against the entire laminin-5 molecule (1:200) (McMillan et al. 2003b). The melanocyte marker antibody TMH-1 recognized the b-locus protein (rat antibody, 1:10 dilution) and was previously described by Masunaga et al. (1996).

Epidermal sections were fixed in cold acetone (−20C) for 10 min and incubated with 5% normal rabbit sera in 0.1 M Dulbecco's PBS for 5 min at 37C. Sections were incubated with primary antibodies and subsequently with secondary antibodies conjugated to fluorescein isothiocyanate or Texas Red (FITC; rabbit anti-mouse IgG or goat anti-rabbit IgG, 1:200; DAKO, Tokyo, Japan; Texas Red conjugated donkey anti-rabbit; Amersham, UK). To label TMH-1, a preabsorbed cyanine (CY5)-conjugated goat anti-rat antibody was used (Jackson ImmunoResearch; West Grove, PA). All secondary antibodies were diluted in 3% BSA in 0.1 M PBS for 30 min at 37C in a darkened, humidified chamber. Sections were then labeled with a ToPro-3 nuclear counterstain (diluted 1:20,000, blue channel; Jackson ImmunoResearch) if appropriate. The sections were then mounted in Permafluor (Thermo Shandon; Pittsburgh, PA) and examined with a confocal microscope (Fluoview FV300; Olympus, Tokyo, Japan) using an inverted microscope (IX70; Olympus). Controls included normal skin cryostat sections with the primary antibody substituted by PBS, myeloma supernatant, or an irrelevant immunoglobulin isotype, as a negative control. All experiments were performed at least in duplicate.

Immunogold Electron Microscopy

Four samples of human skin were cryofixed and processed for postembedding IEM according to the previously described methods (Shimizu et al. 1989,1990). Samples were washed in PBS and cryoprotected in 20% glycerol (in PBS) for up to 1 hr at 4C. Subsequently, cryofixation was performed in liquid propane at −190C using a freeze plunge apparatus (Leica CPC; Cambridge, UK) followed by freeze substitution over 3 days at −80C in methanol using an automated freeze substitution system (AFS; Leica). Specimens were embedded in Lowicryl K11M (Ladd Research Industries; Burlington, VT) resin over 4 days at −60C. The temperature was gradually raised and the resin was polymerized under UV light and liquid nitrogen vapor at 10C. Ultrathin sections were then cut and collected on pioloform-coated nickel grids. Sections were stained with uranyl acetate only (15 min) and observed with a transmission electron microscope (Hitachi H-7100; Tokyo, Japan) at 75 kV. Blocks showing good ultrastructure were selected for immunolabeling experiments. Sections were preincubated in buffer containing PBS with 5% normal goat serum (NGS), 1% BSA, and 0.1% gelatin. Primary antibodies or human antisera were all diluted in PBS buffer containing 1% NGS, 1% BSA, and 0.1% gelatin and incubated at 37C for 2 hr. The sections were then washed in a drop of PBS buffer four times (5 min each) and placed on a drop of secondary linker antibody, again diluted in PBS buffer (for 2 hr at 37C). The secondary antiserum, rabbit anti-mouse IgG (DAKO; Ely, UK) was diluted 1:500. Sections were then incubated with a final antibody layer using 5-nm gold-conjugated labeled goat anti-rabbit or goat anti-mouse antibodies (Biocell; Cardiff, UK) diluted 1:500 in Tris-buffered saline (TBS) for 2 hr at 37C. For double labeling on K11M sections, the α5 chain of laminins 10/11 (4C7 and a 5-nm

gold-conjugated goat anti-mouse) and rabbit anti-laminin 5 (polyclonal highlighted by 15-nm gold-conjugated goat anti-rabbit; Biocell) were used. Sections were washed twice in TBS buffer and twice in distilled water (5 min each). After staining with 15% alcoholic uranyl acetate (3 min) and lead citrate (15 min), sections were observed with a transmission electron microscope (H-7100; Hitachi). Controls included normal skin sections with the primary antibody substituted by PBS, myeloma supernatant, preimmune rabbit serum, or an irrelevant immunoglobulin isotype, as a negative control. All experiments were performed in triplicate.

Immunogold Quantitative Analysis

The techniques for ultrastructural labeling were similar to those performed by McMillan et al. (2003b). Electron micrographs were taken at a standard magnification (30K) and were enlarged by a standard factor ×2.08. The final magnification (×62,500) was checked using electron micrographs taken of a carbon diffraction grating. For standardization purposes, all observations were made by one observer (JRM). At least 200 gold particles were assessed per specimen for each antibody or antiserum and four specimens from different individuals were examined (see Table 1 and Table 2). A 5-nm immunogold-conjugated final antibody layer was used. The percentage of gold particles perpendicularly beneath an observable electron-dense HD cytoplasmic outer attachment plaque as described by McMillan and Eady (1996) was scored and calculated from a large number of gold particles in skin from four individuals.

Only non-obliquely sectioned areas of dermal–epidermal junction were included with clearly defined HD plaques, lamina lucida (LL), and lamina densa (LD). The dermal–epidermal junction beneath melanocytes or in damaged areas was excluded from this study. Gold particles that appeared clumped or associated with any deposit were excluded.

For each antibody or antisera, the positions of gold particles were statistically tested by one-way ANOVA and a two-sample *t*-test using the Minitab statistical package (Minitab Inc; University of Pennsylvania, Philadelphia, PA). An antibody (4C7) that recognizes a carboxyl terminal domain of the α5 chain of laminins 10/11 was used to determine the mean position of labeling directly beneath the keratinocyte plasma membrane (Engvall et al. 1986; Makino et al. 2002)(see Figure 1 for epitope position). The labeling of the α5 chain was compared with the distribution of the G1 domain of laminin-5 α3 chain (using data previously reported by McMillan et al. 2003b).

Results

Confocal Fluorescence Microscopy of Control Skin

Laminin-5 staining was restricted to the dermal–epidermal junction in control skin (data not shown). This was similar to the dermal–epidermal junction staining of α5 chain of laminins 10 (data not shown). Laminins 10 and 11 were also expressed in dermal blood vessels. Laminin 11 (as identified by the β2 chain) dermal–epidermal junction staining was present in adult control thigh and arm skin but was variable in other samples including scalp skin. Therefore, β2 chain expression appears to be distinct and independent from that of the α5 chain. Staining for the α5, β1, and γ1 chains was weaker in the adult dermal–epidermal junction than in blood vessels (data not shown), whereas dermal–epidermal junction staining was generally brighter in younger skin samples (<16 years, data not shown). This would appear to support a previous report of age-dependent expression of the laminin 10/11 chains (Pouliot et al. 2002).

Confocal fluorescence microscopy (Figures 2A–2C) showed that both laminin-5 and α5 chains are expressed in the dermal–epidermal junction of control interfollicular epidermis except for small gaps (white arrows in Figures 2A and 2B) beneath small isolated cells presumed to be melanocytes staining blue for the melanocyte marker, TMH-1 (Figures 2A and 2B) (Masunaga et al. 1996). These data suggest that laminin-10 chains are restricted to beneath keratinocytes and are not expressed beneath melanocytes.

A previous scalp skin and hair follicle immunohistochemical study (Akiyama et al. 1995) demonstrated a specific staining pattern for many HD and anchoring filament components, particularly laminin 5, which manifests as reduced staining around the lower hair bulb and a reemergence of staining over the dermal papilla region (Akiyama et al. 1995). We observed this

Table 2 Immunogold particle distribution shows the majority of laminin labeling is restricted to beneath the hemidesmosome (HD) plaque

Antibody/antisera	Recognizes chain and epitope	Present in which chain/isoform(s)	Number of skin samples	Frequency of gold particles under HDs % (±SD)
Laminin 5	All chains[a]	Lam 5[a]	2[a]	77–88[a]
BM-165	α3 chain	Lam 5/6	4	82.65 (±3.87)
4C7	α5 chain	Lam 10/11	4	84.3 (±3.89)
2E8	β1 chain	Lam 6/10	4	91.7 (±3.99)
C4	β2 chain	Lam 7/11	4	88.4 (±3.56)
D18	γ1 chain	Lam 6/7/10/11	4	92.0 (±2.65)
M3F7	Collagen IV	α1/α2 helical (IV)	4	61.3 (±3.05)

[a]Data from McMillan et al. 2003b and Masunaga et al. 1996.

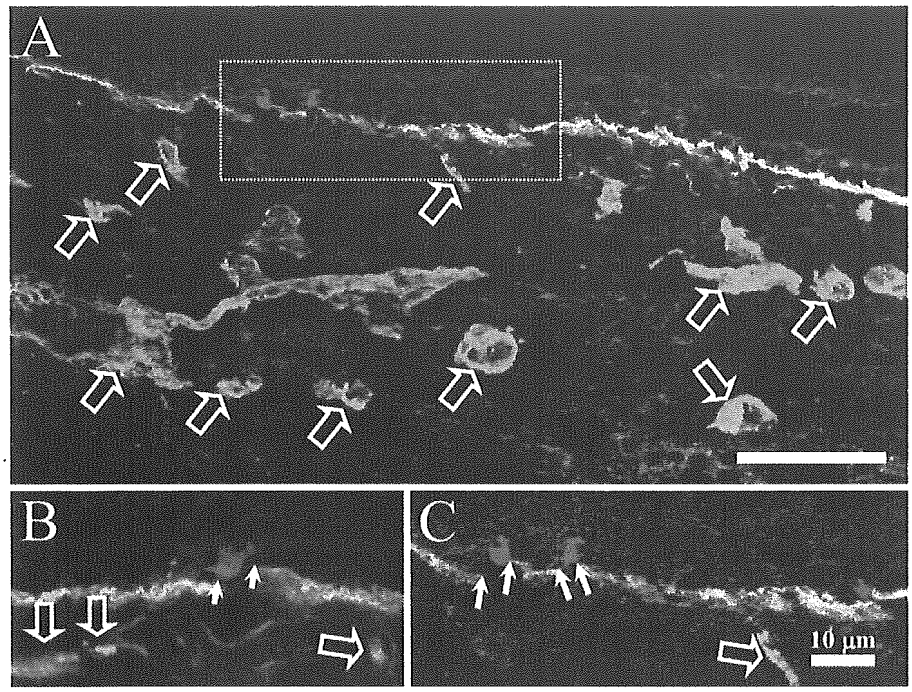

Figure 2 Reduced laminin 10 (green, FITC) and laminin 5 (red, Texas Red) labeling below the melanocyte marker TMH-1 (blue, CY-5) of normal adult control skin. Both laminin 5 and the α5 chain colocalize (orange color) within the dermal–epidermal junction (**A**) and both are expressed only weakly or are absent beneath melanocytes (**B,C**, in blue, see white arrows). The α5 chain of laminins 10/11 together with laminin 5 is not expressed beneath melanocytes (**A–C**, white arrows) but does show a distinct, strong expression pattern that includes dermal vessels (**A–C**, open arrows). Bar = 25 μm; Inset **C** = 10 μm.

characteristic pattern of staining along the majority of the follicles, for both laminin 5 (bracketed area in Figure 3A) and the laminin α5 chain (brackets and dotted line in Figures 3B and 3D). The laminin β1 and γ1 chains also showed this staining pattern (data not shown). There was no staining for the β2 chain in the hair follicle (data not shown). The dermal–epidermal junction of the bulge region stained for both α3 and the α5 chains (Figures 3A and 3B, Bu) and the α5 chain also stained the erector pili muscle (Figure 3C, EP).

Confocal Fluorescence Microscopy of Epidermolysis Bullosa Skin

The expression of laminins 5 (γ2 chain), 10 (all chains), and 11 (β2 chain) in patients with different forms of EB

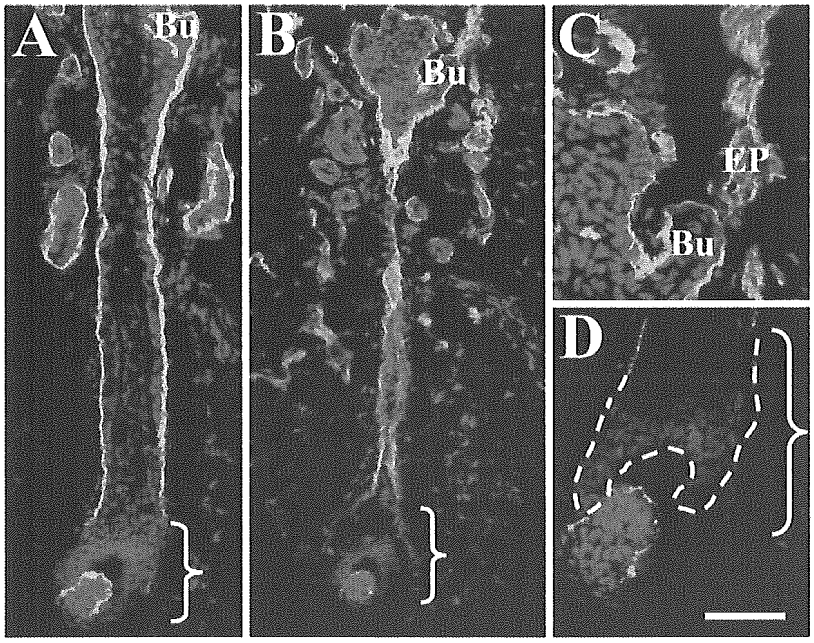

Figure 3 Indirect immunofluorescence shows a typical hemidesmosomal (HD) component-like expression pattern of the laminin α5 chain in late anagen human hair follicles. A previous scalp hair follicle immunohistochemical study (Akiyama et al. 1995) demonstrated a specific staining pattern for many HD-anchoring filament-associated components including laminin 5. In our study, both laminin-5 polyclonal staining (**A**) and the laminin α5 chain (**B**, 4C7) showed characteristic bright patterns along the epidermal proximal hair shaft including the bulge region (**B,C**, Bu) but progressively weaker staining toward the hair bulb (**D**, bracketed areas) with staining becoming brighter again higher up the hair shaft. Laminin α5 chain staining was present in the shaft (**B**) bulge region (**B,C**) and the apical tip of the hair bulb matrix (**D**). Laminin β1 and γ1 chains showed similar staining to the α5 chain (data not shown). No laminin β2 chain staining was detected in the hair follicle (data not shown). Bar = 25 μm.

was compared. In both control (Figure 4A) and all of the EB subtypes (Figures 4B–4H), α5, β1, β2, and γ1 chain expression was detectable. Laminin expression was weak in areas of split skin particularly in HJEB with defects in laminin 5 (α5 chain, Figures 4B and 4C, respectively, asterisks show the split area) (Uitto and Pulkkinen 2001). The reduction in α5 and β2 chain expression in HJEB patients, particularly over split skin,

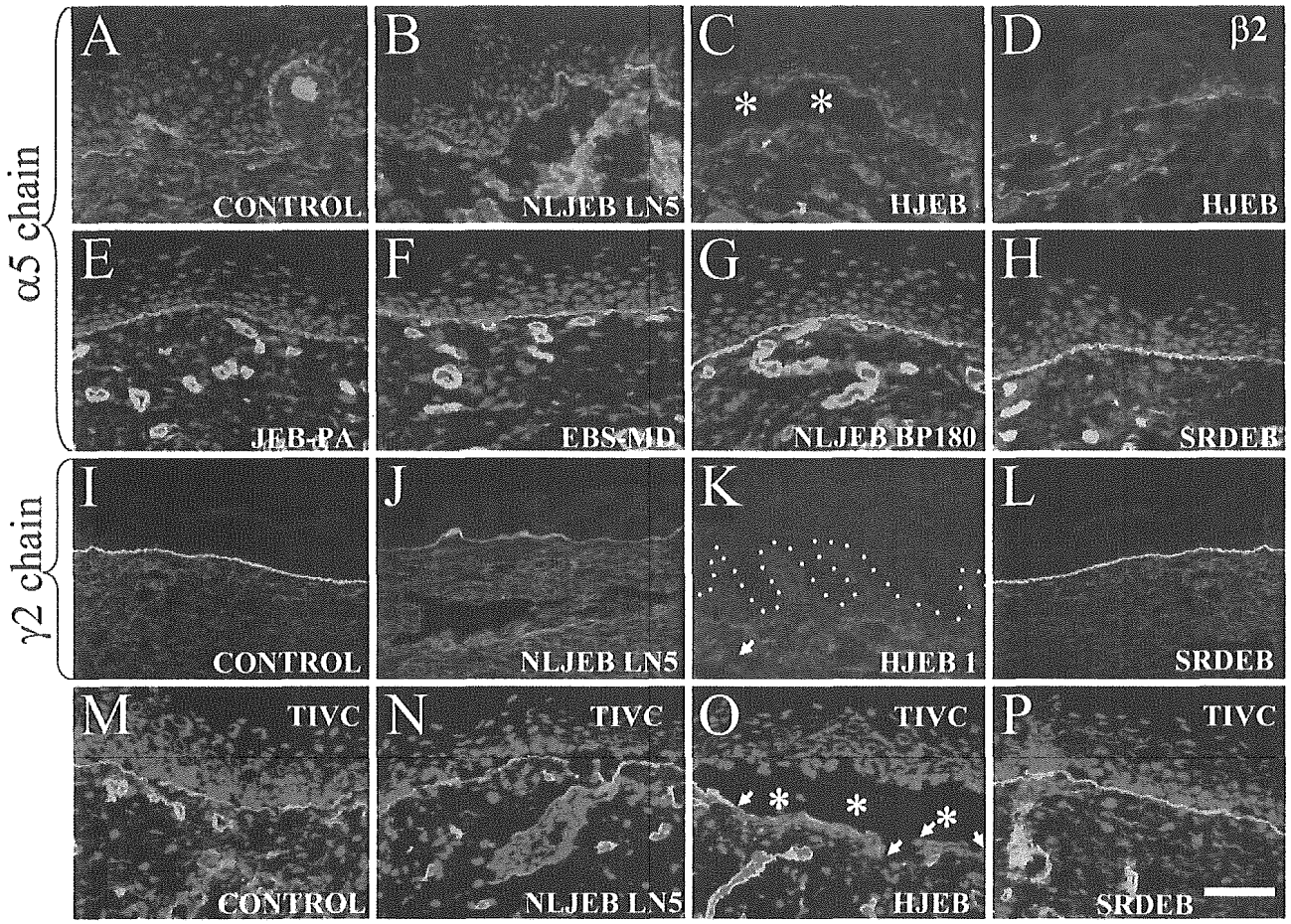

Figure 4 Laminin α5 and β2 chains are expressed beneath the epidermis in epidermolysis bullosa (EB) skin but are focally reduced in split lethal Herlitz junctional EB (HJEB) skin. The laminin α5 chain in control skin showed linear fluorescence along the dermal–epidermal junction and in dermal blood vessels (**A**). However, in non-lethal (**B**) and HJEB skin (**C,D**), the laminin α5 and β2 chains showed reductions in dermal–epidermal junction staining, especially where areas of skin had become separated (**C**, asterisks). This effect was due to antigen degradation in HJEB skin during skin separation as demonstrated by reduced collagen IV staining (**O**, arrows:) over the split areas (**O**, asterisks), whereas control skin (**M**), non-lethal junctional EB (NLJEB) (**N**) and dystrophic EB skin (**P**) showed bright linear collagen IV staining, respectively. The presence of α5 and β2 chain staining in intact EB skin demonstrates that these chains are independently synthesized and maintained even in the presence of other defective basement membrane components. All other cases of EB showed normal staining for the laminin α5 chain (and β2 chain, not shown), including junctional EB associated with pyloric atresia (JEB-PA with defects in α6β4 integrin (**E**), EB simplex associated with muscular dystrophy (EBS-MD with defects in plectin) (**F**), NLJEBBP180 with defects in BP180 (**G**), and severe recessive dystrophic EB (SRDEB with collagen VII defects (**H**). In control and SRDEB patients' skin, laminin-5 γ2 chains were normally expressed (**I** and **L**, respectively) using the γ2 chain monoclonal antibody GB3. Laminin-5 expression was severely reduced and absent in both the NLJEB and HJEB cases (**J,K**), respectively, harboring severe defects in laminin 5. Bar = 50 μm.

Figure 5 The majority of laminin 5 and laminin 10/11 chains are restricted to the lamina densa beneath HDs, whereas collagen IV is expressed continuously along the basal lamina. Postembedding immunoelectron microscopy with anti-α5 chain (laminin 10) (**A–D**) and double labeling with anti-α3 chain (laminin 5) (**E**) antibodies in control skin reveals a similar labeling pattern for these laminins. Collagen IV (M3F7), however, is not restricted to beneath HDs but is continuous along the basal lamina (**F**). Double labeling with laminin 5 polyclonal antiserum (15 nm gold particles) and laminin 10/11 (with smaller 5 nm gold particles) shows that the majority of labeling colocalizes beneath HDs at the border between the lamina lucida and lamina densa (**E**). The majority (84%) of laminin α5 chain labeling (see Table 2 and **A–D**) was restricted to areas immediately beneath the HDs, over the LD border (**A–D**, arrows) whereas only 61% of collagen IV was restricted to beneath HDs (**F**). HD plaques (solid arrows) are shown within the keratinocyte cytoplasm (white cross) and the lamina lucida highlighted by asterisks. Bar = 0.2 μm.

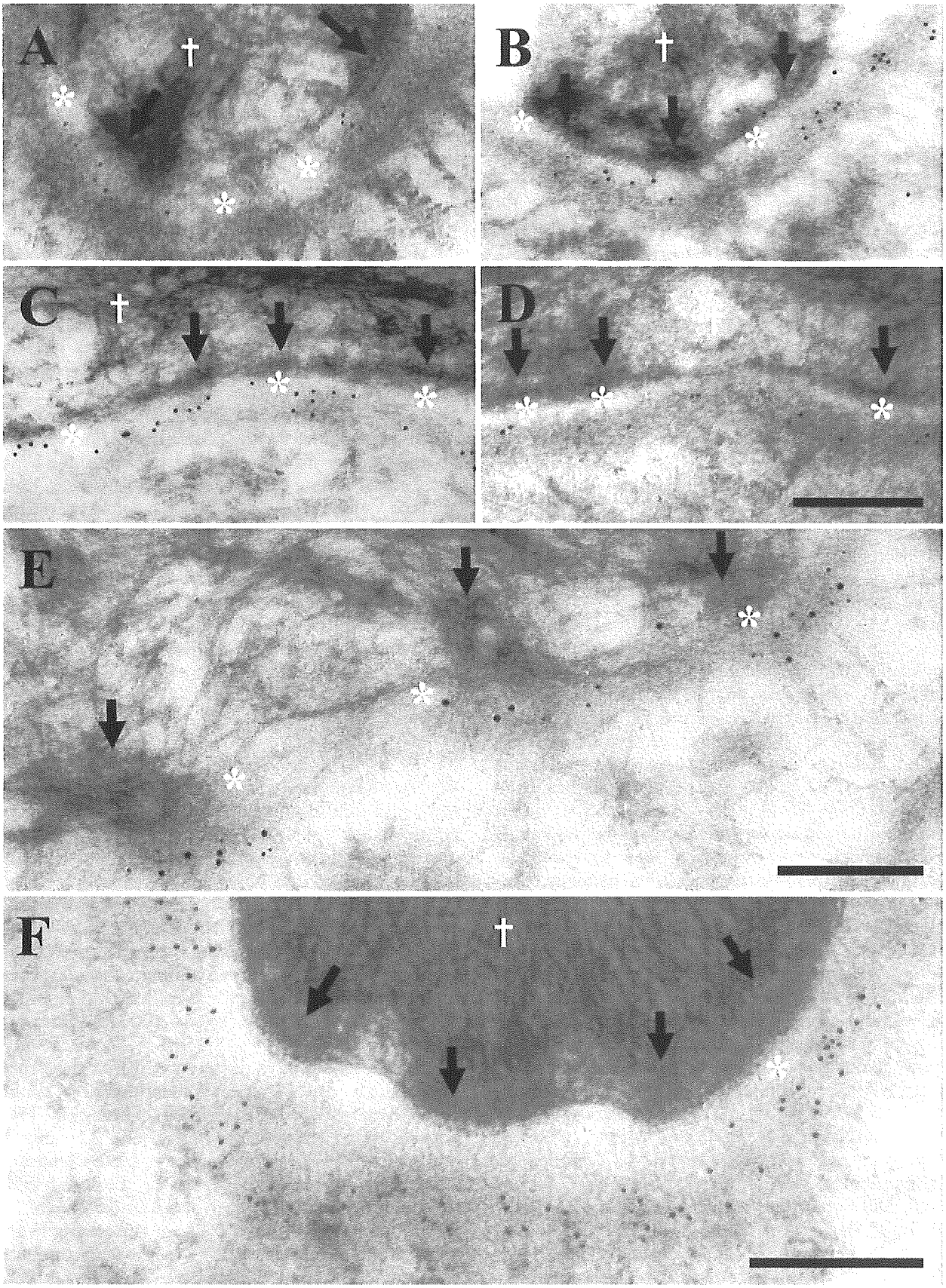

suggested that this effect might be due to antigen degradation in vivo in the split areas. The presence of α5 and β2 chains in intact EB skin, however, confirms that these chains are capable of being independently synthesized and assembled even in the total absence or in the presence of defective laminin 5. All other EB cases also showed normal staining for other laminins including junctional EB associated with pyloric atresia (JEB-PA) (with defects in α6β4 integrin, Figure 4E), EB simplex associated with muscular dystrophy (EBS-MD) (with defects in plectin, Figure 4F), non-lethal junctional (NLJEB) (with defects in BP180, Figure 4G), and severe recessive dystrophic epidermolysis bullosa (SRDEB) (Figure 4H). In control and SRDEB patients' skin there was normal staining for laminin 5 (γ2 chain using the antibody GB3, see Figure 4L). This was in contrast to laminin-5 chain staining that was severely reduced or absent in both the NLJEB (Figure 4J) and HJEB cases (Figure 4K), harboring severe defects in laminin-5 expression.

Immunogold Electron Microscopy and Quantitative Analysis

Labeling of control interfollicular epidermal sections showed that the majority of laminin-10 α5 chains (Figures 5A–5D; Table 2), β1, γ1, and 11 chain (β2 chain, data not shown) were restricted to under the cytoplasmic HD outer plaques. This was in contrast to collagen IV, which was not as restricted to beneath epidermal HDs plaques (see Figure 5F, 61% collagen IV vs 82% laminin 5). The difference between all laminin and collagen values was statistically significant using the one-way ANOVA ($p<0.001$) and Student's t-test ($p<0.000$). All four α5, β1, β2, and γ1 chain antibodies and antiserum showed a remarkable similarity in the percentage of labeling associated with the HD attachment plaque and anchoring filament complex beneath HDs, ranging between 84% and 92% (see Table 2). Furthermore, these values reflect an almost identical (HD restricted) expression pattern to the previously reported values for laminin-5 subunits (Masunaga et al. 1996; McMillan et al. 2003b) (part of these findings are also included in Table 2). Our data are very similar to those of laminin 5 (α3 chain) that on average demonstrated 82% of labeling restricted to beneath HDs (see Table 2) at a distance ranging from 35 to 45 nm below the plasma membrane at the LL–LD junction (Masunaga et al. 1996; McMillan et al. 2003b). The precise distance of the 4C7 epitope on the C-terminal portion of the α5 chain was 53.07 nm (±6.69 SD) from the plasma membrane (arrows, Figures 5A–5D). This is 18 nm lower than the G1 domain of the laminin-5 α3 chain described previously (see Figure 1) (McMillan et al. 2003b). The difference between these two α chain mean values was statistically significant using the one-way ANOVA ($p>0.01$) and Student's t-test ($p=0.009$). However, visual examination of the distribution of these two antigens revealed overlapping values ~30–40 nm beneath the plasma membrane, the only difference being that the α5 chain showed a wider range of labeling that extended deeper in the LD compared with the α3 chain. The remaining three β1-, β2-, and γ1-chain antibodies recognized, as yet unidentified, epitopes on specific laminin chains and were therefore not included in the plasma membrane distance measurements. However, all three antibodies showed upper LD labeling (not shown), the majority of which were restricted to beneath HDs similar to the α5 chain. The three β1-, β2-, and γ1-chain antibodies were excluded from the distance measurements but were scored for their localization either beneath visible HD attachment plaques (as defined by McMillan and Eady 1996) or within inter-HD areas.

Double labeling for the α5 chain of laminins 10/11 (highlighted by 5-nm small gold particles) and whole anti-laminin 5 antiserum (shown by the larger 15-nm gold particles) shows a similar labeling pattern in the LD beneath electron densities presumed to be HDs (Figure 5E). HD plaques are visible within the keratinocyte cytoplasm (white cross) and the dermal–epidermal junction is separated by the LL (Figure 5E, asterisks). Together our data suggest that the α5 chains (including β1, β2, and γ1 chains, see Table 2) show a restricted expression pattern beneath HDs, similar to laminin 5 but unlike collagen IV.

Discussion

We have demonstrated that the α5, β1, and γ1 chains show a similar localization to laminin 5 in the human interfollicular epidermal basement membrane. These data support the presence of multiple laminin isoforms beneath HDs in the basement membrane at several different epidermal sites. A very different localization of collagen IV within the LD but not restricted to beneath HDs was observed. These data suggest a complex network of interactions between different basement membrane components beneath the epidermis (Ghohestani et al. 2001; McMillan et al. 2003a; Miner and Yurchenco 2004).

In addition we have demonstrated that the expression of the α5 and β2 chains is independent of laminin 5, as demonstrated by residual staining in HJEB patients' skin. The reduction in α5 and β2 chain expression in HJEB was only observed over separated, blistered areas of skin, suggesting that this effect is due to separation-induced antigen degradation in vivo. This was supported by reduced collagen IV staining in split areas of EB skin. This was confirmed after reduced collagen IV staining was observed within separated areas of HJEB skin samples (data not shown). Our

results also suggest that the presence of other laminins cannot fully compensate for defects in laminin-5-deficient HJEB skin (McMillan et al. 1997,1998). The α5 and β2 chains were also normally expressed in all other EB samples harboring defects in plectin, collagen XVII (bullous pemphigoid antigen 2), the α6β4 integrin, and collagen VII.

In previous reports (Aumailley and Rousselle 1999), the laminin β2 chain was not expressed in the epidermal basement membrane of neonatal foreskin. However, we showed weak, variable β2 chain expression (in thigh and arm skin) and absences in other body sites (scalp skin). We conclude that the lack of β2 staining may be due to several factors: antigen masking, a low-level expression, or site- or age-specific variations in human laminin β2 chain expression that may include posttranslational protein processing seen in other laminin isoforms (Miner et al. 1997).

Laminin 5, together with several HD-associated antigens, is expressed in a specific pattern around late anagen hair follicles that excludes staining around the dermal papilla area (Akiyama et al. 1995; Nutbrown and Randall 1995). Laminin-10 chains also show this similar expression pattern in late anagen hair follicles. Unlike laminin-5 and laminin-10 chains, we failed to observe any β2 chain expression (laminins 7/11) in any part of the adult hair follicle; however, this may be due to a low level of antigen expression or masking of the β2 chain epitope. The significance of these findings may be related to the specific growth phases of the lower non-permanent portion of the hair follicle.

In the laminin α5 chain knockout mouse, an unusual disruption in hair follicle morphogenesis was demonstrated (Li, et al., 2003). Li et al. (2003) reported that, in control mice, laminin 10 was present in murine elongating hair germs when other laminins were down-regulated, suggesting a specific role for this laminin in hair follicle development and follicular keratinocyte migration. Mouse skin lacking laminin 10 also contained fewer hair germs and follicles compared with control mice, and after transplantation experiments this skin showed a failure of hair germ elongation and defective basement membrane assembly. Intriguingly, treatment of these mice with purified exogenous laminin 10 corrected these defects and restored hair follicle development. Given that human hair follicles are slow cycling and the majority remains in the late anagen phase and shows different growth characteristics to murine follicles, our failure to demonstrate such growth phase-specific differences in the expression of laminin 10 during the hair cycle stages is not surprising.

The presence of multiple laminin isoforms beneath HDs suggests the hypothesis that there are laminin subunits possibly with overlapping functions that form focal clusters of laminin molecules. This was in contrast to collagen IV, which was not restricted to HDs and localized to the LD region. Ultrastructural data show that the α3 chain (laminin 5) is closer to the plasma membrane than the α5 chain (with only an 18-nm difference, see Table 2). This might suggest that the α5 chain is more closely associated with a LD component such as collagen IV. However, given the size of both laminin chains of ~80–100 nm (as determined by rotary shadowing experiments), our data suggest a significant overlap occurs between α3 and α5 chains (Marinkovich et al. 1992; Vailly et al. 1994). Further studies using a larger battery of antibodies are required to determine the orientation of these laminin components.

Together these data show for the first time that laminin 10/11 chains are restricted to beneath HDs similar to laminin 5 but distinct from collagen IV. Our data suggest a specific localization of multiple laminin isoforms in the epidermal basement membrane beneath HDs and support the hypothesis that several laminins in close association may promote stable cell attachment among different basement membrane molecules.

Acknowledgments

This work was supported by a grant-in-aid of Scientific Research A (13357008, HS) and Health and Labor Sciences Research Grants (Research into Specific Diseases) H13-Saisei-02 and H17-Saisei 12, by a grant from the Japanese Society for the Promotion of Science (JSPS) grant #00345 to J.R.M., and by a grant-in-aid for JSPS fellows' research expenses (#00345). This work was also supported by a grant from the Japanese Health Science Foundation for Research Residents, for class "A" researchers (JRM).

We gratefully acknowledge the technical support of Ms. M. Sato and Ms. K. Sakai in this study. We also thank Dr. T. Masunaga for kindly providing the data from the γ2 chain study (Masunaga et al. 1996) and Dr. M.P. Marinkovich for his kind gift of his polyclonal laminin 5 antibody. Hybridoma supernatants D18 and 2E8 (produced by Drs. J. Sanes and E. Engvall) and M3F7 (from Dr. H. Furthmeyer) were obtained from the Developmental Studies Hybridoma Bank, developed under the auspices of the National Institute of Child Health and Human Development (NICHD) and maintained by the University of Iowa, Department of Biological Sciences, Iowa City, Iowa.

Literature Cited

Akiyama M, Dale BA, Sun TT, Holbrook KA (1995) Characterization of hair follicle bulge in human fetal skin: the human fetal bulge is a pool of undifferentiated keratinocytes. J Invest Dermatol 105: 844–850

Aumailley M, Rousselle P (1999) Laminins of the dermo-epidermal junction. Matrix Biol 18:19–28

Engvall E, Davis GE, Dickerson K, Ruoslahti E, Varon S, Manthorpe M (1986) Mapping of domains in human laminin using monoclonal antibodies: localization of the neurite-promoting site. J Cell Biol 103:2457–2465

Engvall E, Earwicker D, Haaparanta T, Ruoslahti E, Sanes JR (1990) Distribution and isolation of four laminin variants; tissue restricted distribution of heterotrimers assembled from five different subunits. Cell Regul 1:731–740

Foellmer HG, Madri JA, Furthmayr H (1983) Methods in laboratory investigation. Monoclonal antibodies to type IV collagen: probes

for the study of structure and function of basement membranes. Lab Invest 48:639–649
Geuijen CA, Sonnenberg A (2002) Dynamics of the α6β4 integrin in keratinocytes. Mol Biol Cell 13:3845–3858
Ghohestani RF, Li K, Rousselle P, Uitto J (2001) Molecular organization of the cutaneous basement membrane zone. Clin Dermatol 19:551–562
Gu J, Sumida Y, Sanzen N, Sekiguchi K (2001) Laminin-10/11 and fibronectin differentially regulate integrin-dependent Rho and Rac activation via p130(Cas)-CrkII-DOCK180 pathway. J Biol Chem 276:27090–27097
Hunter DD, Shah V, Merlie JP, Sanes JR (1989) A laminin-like adhesive protein concentrated in the synaptic cleft of the neuromuscular junction. Nature 338:229–234
Kennedy AR, Heagerty AH, Ortonne JP, Hsi BL, Yeh CJ, Eady RA (1985) Abnormal binding of an anti-amnion antibody to epidermal basement membrane provides a novel diagnostic probe for junctional epidermolysis bullosa. Br J Dermatol 113:651–659
Kikkawa Y, Sanzen N, Fujiwara H, Sonnenberg A, Sekiguchi K (2000) Integrin binding specificity of laminin-10/11: laminin-10/11 are recognized by α3β1, α6β1 and α6β4 integrins. J Cell Sci 113:869–876
Kikkawa Y, Sanzen N, Sekiguchi K (1998) Isolation and characterization of laminin-10/11 secreted by human lung carcinoma cells. Laminin-10/11 mediates cell adhesion through integrin α3β1. J Biol Chem 273:15854–15859
Li J, Tzu J, Chen Y, Zhang YP, Nguyen NT, Gao J, Bradley M, et al. (2003) Laminin-10 is crucial for hair morphogenesis. EMBO J 22: 2400–2410
Makino M, Okazaki I, Kasai S, Nishi N, Bougaeva M, Weeks BS, Otaka A, et al. (2002) Identification of cell binding sites in the laminin α5-chain G domain. Exp Cell Res 277:95–106
Marinkovich MP, Lunstrum GP, Burgeson RE (1992) The anchoring filament protein kalinin is synthesized and secreted as a high molecular weight precursor. J Biol Chem 267:17900–17906
Masunaga T, Shimizu H, Ishiko A, Tomita Y, Aberdam D, Ortonne JP, Nishikawa T (1996) Localization of laminin-5 in the epidermal basement membrane. J Histochem Cytochem 44:1223–1230
McMillan JR, Akiyama M, Shimizu H (2003a) Epidermal basement membrane zone components: ultrastructural distribution and molecular interactions. J Dermatol Sci 31:169–177
McMillan JR, Akiyama M, Shimizu H (2003b) Ultrastructural orientation of laminin 5 in the epidermal basement membrane: an updated model for basement membrane organization. J Histochem Cytochem 51:1299–1306
McMillan JR, Eady RA (1996) Hemidesmosome ontogeny in digit skin of the human fetus. Arch Dermatol Res 288:91–97
McMillan JR, McGrath JA, Pulkkinen L, Kon A, Burgeson RE, Ortonne J-P, Meneguzzi G, et al. (1997) Immunohistochemical analysis of skin in junctional epidermolysis bullosa using laminin 5 chain specific antibodies is of limited value in predicting the underlying gene mutation. Br J Dermatol 136:817–822
McMillan JR, McGrath JA, Tidman MJ, Eady RA (1998) Hemidesmosomes show abnormal association with the keratin filament network in junctional forms of epidermolysis bullosa. J Invest Dermatol 110:132–137
Mercurio AM, Rabinovitz I, Shaw LM (2001) The α6β4 integrin and epithelial cell migration. Curr Opin Cell Biol 13:541–545
Miner JH, Patton BL, Lentz SI, Gilbert DJ, Snider WD, Jenkins NA, Copeland NG, et al. (1997) The laminin α chains: expression, developmental transitions, and chromosomal locations of α1–5, identification of heterotrimeric laminins 8–11, and cloning of a novel α3 isoform. J Cell Biol 137:685–701
Miner JH, Yurchenco PD (2004) Laminin functions in tissue morphogenesis. Annu Rev Cell Dev Biol 20:255–284
Niessen CM, Hogervorst F, Jaspars LH, de Melker AA, Delwel GO, Hulsman EH, Kuikman I, et al. (1994) The α6β4 integrin is a receptor for both laminin and kalinin. Exp Cell Res 211:360–367
Nishiyama T, Amano S, Tsunenaga M, Kadoya K, Takeda A, Adachi E, Burgeson RE (2000) The importance of laminin 5 in the dermal-epidermal basement membrane. J Dermatol Sci 24(suppl 1): S51–59
Nutbrown M, Randall VA (1995) Differences between connective tissue-epithelial junctions in human skin and the anagen hair follicle. J Invest Dermatol 104:90–94
Pouliot N, Saunders NA, Kaur P (2002) Laminin 10/11: an alternative adhesive ligand for epidermal keratinocytes with a functional role in promoting proliferation and migration. Exp Dermatol 11: 387–397
Pulkkinen L, Smith FJ, Shimizu H, Murata S, Yaoita H, Hachisuka H, Nishikawa T, et al. (1996) Homozygous deletion mutations in the plectin gene (PLEC1) in patients with epidermolysis bullosa simplex associated with late-onset muscular dystrophy. Hum Mol Genet 5:1539–1546
Sanes JR, Engvall E, Butkowski R, Hunter DD (1990) Molecular heterogeneity of basal laminae: isoforms of laminin and collagen IV at the neuromuscular junction and elsewhere. J Cell Biol 111: 1685–1699
Shimizu H, McDonald JN, Gunner DB, Black MM, Bhogal B, Leigh IM, Whitehead PC, et al. (1990) Epidermolysis bullosa acquisita antigen and the carboxy terminus of type VII collagen have a common immunolocalization to anchoring fibrils and lamina densa of basement membrane. Br J Dermatol 122:577–585
Shimizu H, McDonald JN, Kennedy AR, Eady RAJ (1989) Demonstration of intra- and extra-cellular localization of bullous pemphigoid antigen using cryofixation and freeze substitution for postembedding immuno-electron microscopy. Arch Dermatol Res 281:443–448
Takizawa Y, Pulkkinen L, Shimizu H, Lin L, Hagiwara S, Nishikawa T, Uitto J (1998a) Maternal uniparental meroisodisomy in the LAMB3 region of chromosome 1 results in lethal junctional epidermolysis bullosa. J Invest Dermatol 110:828–831
Takizawa Y, Shimizu H, Pulkkinen L, Hiraoka Y, McGrath JA, Suzumori K, Aiso S, et al. (1998b) Novel mutations in the LAMB3 gene shared by two Japanese unrelated families with Herlitz junctional epidermolysis bullosa, and their application for prenatal testing. J Invest Dermatol 110:174–178
Takizawa Y, Shimizu H, Pulkkinen L, Nonaka S, Kubo T, Kado Y, Nishikawa T, et al. (1998c) Novel premature termination codon mutations in the laminin γ2-chain gene (LAMC2) in Herlitz junctional epidermolysis bullosa. J Invest Dermatol 111:1233–1234
Takizawa Y, Shimizu H, Pulkkinen L, Suzumori K, Kakinuma H, Uitto J, Nishikawa T (1998d) Combination of a novel frameshift mutation (1929delCA) and a recurrent nonsense mutation (W610X) of the LAMB3 gene in a Japanese patient with Herlitz junctional epidermolysis bullosa, and their application for prenatal testing. J Invest Dermatol 111:1239–1241
Tiger CF, Champliaud MF, Pedrosa-Domellof F, Thornell LE, Ekblom P, Gullberg D (1997) Presence of laminin α5 chain and lack of laminin α1 chain during human muscle development and in muscular dystrophies. J Biol Chem 272:28590–28595
Uitto J, Pulkkinen L (2001) Molecular genetics of heritable blistering disorders. Arch Dermatol 137:1458–1461
Vailly J, Verrando P, Champliaud MF, Gerecke D, Wagman DW, Baudoin C, Aberdam D, et al. (1994) The 100-kDa chain of nicein/kalinin is a laminin B2 chain variant. Eur J Biochem 219: 209–218
Yu H, Talts JF (2003) β1 Integrin and α-dystroglycan binding sites are localized to different laminin-G-domain-like (LG) modules within the laminin α5 chain G domain. Biochem J 371:289–299

The Journal of Histochemistry & Cytochemistry

Simultaneous application of basic fibroblast growth factor and hepatocyte growth factor to enhance the blood vessels formation

Akira Marui, MD,[a] Akihiro Kanematsu, MD, PhD,[b] Kenichi Yamahara, MD, PhD,[c] Kazuhiko Doi, MD,[d] Toshihiro Kushibiki, MS,[b] Masaya Yamamoto, PhD,[b] Hiroshi Itoh, MD, PhD,[c] Tadashi Ikeda, MD, PhD,[a] Yasuhiko Tabata, PhD, DMSc, DPharm,[b] and Masashi Komeda, MD, PhD,[a] *Koyoto, Japan*

Objective: The present study investigated whether the simultaneous application of basic fibroblast growth factor (bFGF) and hepatocyte growth factor (HGF) enhances blood vessel formation in murine ischemic hindlimb compared with bFGF or HGF applied alone.

Methods: Unilateral hindlimb ischemia was created in C57BL/6 mice. Hindlimb blood flow was evaluated by laser Doppler perfusion image index (LDPII) (ratio (%) of ischemic-to-normal-limb blood flow). The ischemic limbs were treated with bFGF and HGF separately, or bFGF and HGF together, and their therapeutic effects were assessed. Collagen microspheres (CM) were used as a sustained-release carrier for bFGF and HGF.

Results: A single intramuscular injection of 5 μg or less of bFGF-incorporated CM (bFGF/CM) into the ischemic limb did not significantly increase the LDPII compared with the control (no treatment) 4 weeks after the treatment. Similarly, 20 μg or less of HGF/CM did not increase LDPII. Based on these results, we compared the dual release of CM incorporating 5 μg of bFGF and 20 μg of HGF with either the single release of 5 μg of bFGF/CM alone or 20 μg of HGF/CM alone. The LDPII of the dual release (94.2% ± 10.9%) was higher than either single release (51.2% ± 5.8% or 52.5% ± 8.0%, $P < .01$). Furthermore, the LDPII in the dual release (94.2% ± 10.9%) was equivalent to that with 80 μg of bFGF/CM (95.1% ± 7.6%) alone or 80 μg of HGF/CM (92.8% ± 7.6%) alone. A histologic evaluation at 4 weeks showed capillary density in the dual release (868 ± 173 vessels/mm^2) was higher than that in either single release (204 ± 68 vessels/mm^2 or 185 ± 98 vessels/mm^2, $P < .01$). The percentage of mature vessels assessed by α-smooth muscle actin staining was also higher in the dual release (43.8% ± 7.8% vs 9.5% ± 3.0% or 11.7% ± 3.8%, respectively; $P < .01$).

Conclusions: This study demonstrates that the sustained dual release of a lower dose of bFGF and HGF from a carrier matrix can achieve equivalent blood perfusion recovery and more mature vasculature in the ischemic limb than a higher dose of bFGF or HGF alone. This approach may be a highly promising strategy for the future treatment of peripheral vascular disease. (J Vasc Surg 2005;41:82-90.)

Clinical Relevance: Clinical trials of growth-factor therapies for ischemia have revealed several problems, such as immature vasculature, adverse effects of high-dose growth factors, or immune and inflammatory responses of viral vectors. This study demonstrates that the sustained dual release of lower-dose basic fibroblast growth factor (bFGF) and hepatocyte growth factor (HGF) from biodegradable collagen microspheres (CM) can achieve equivalent blood perfusion recovery and more mature vasculature in ischemic limb than higher-dose bFGF or HGF alone. CM does not aggravate focal inflammation in the ischemic limb. This approach may be a highly promising strategy for the future treatment of peripheral vascular disease.

The development of growth-factor therapy has shown encouraging results in various clinical studies in cardiovascular field.[1-4] However, there are still unignorable concerns for unstable and immature vasculature, adverse effects of high-dose growth factors, and immune or inflammatory responses of viral vectors.[5-8] Specifically, prolonged exposure of skeletal muscle or myocardium to high local levels of vascular endothelial growth factor (VEGF) or the fibroblast growth factor (FGF) family of peptides can cause hemangioma-like tumors, vascular malformations, and neointimal development.[5-8] To minimize such adverse effects, dose-reduction of these angiogenic growth factors would be an important strategy in this field.

Combination therapy is a common way to obviate dose escalation of a single agent in multiple clinical areas such as antihypertensive therapy or cancer chemotherapy. In areas

From the Departments of Cardiovascular Surgery,[a] and Medicine and Clinical Science,[c] Kyoto University Graduate School of Medicine, and Department of Biomaterials, Institute for Frontier Medical Sciences, Kyoto University[b] and Takeda Hospital.[d]

Competition of interest: none.

Supported by a Grant for Scientific Research, from the Japanese Ministry of Education and Science.

Reprint requests: Masashi Komeda, MD, PhD, Professor and Chairman, Department of Cardiovascular Surgery, Kyoto University Graduate School of Medicine, 54 Shogoin Kawahara, Sakyo, Kyoto, Japan 606-8507 (e-mail: masakom@kuhp.kyoto-u.ac.jp)

0741-5214/$30.00

doi:10.1016/j.jvs.2004.10.029